

Changes in the proliferative capacity of NG2 cell subpopulations during postnatal development of the mouse hippocampus

Behrouz Moshrefi-Ravasdjani¹ · Pavel Dublin¹ · Gerald Seifert² · Katja Jennissen² · Christian Steinhäuser² · Karl W. Kafitz¹ · Christine R. Rose¹

Received: 10 March 2016 / Accepted: 5 June 2016 / Published online: 15 June 2016
© Springer-Verlag Berlin Heidelberg 2016

Abstract Besides astrocytes and oligodendrocytes, NG2 proteoglycan-expressing cells (NG2 glia) represent a third subtype of macroglia in the brain. Originally described as oligodendrocyte precursor cells, they feature several characteristics not expected from mere progenitor cells, including synaptic connections with neurons. There is accumulating evidence that the properties of NG2 glia differ between different brain regions and developmental stages. To further analyze this proposed heterogeneity, we studied electrophysiological properties, transcript and protein expression, distribution and proliferative capacity of NG2 glia during postnatal development, focusing on the hippocampus and corpus callosum. All NG2 glia displayed a ‘complex’ current pattern consisting of voltage- and time-dependent in- and outward currents. In juvenile mice, Kir current densities and rectification index were highly variable and on average significantly lower than in adult animals. Single cell RT-PCR analyses of electrophysiologically characterized cells demonstrated that different glial genes were expressed at variable extent, independent of developmental stage and genetic background. In the hippocampus proper and the corpus callosum, the density of NG2 glia was

highest at postnatal days (P)10–12, decreased by ~50 % at P25–35 and then remained stable in adults (P80–90). Interestingly, co-expression of NG2 and S100 β , a marker for mature astrocytes, increased from 7 % at P10–12 to 27 % at P25–35 in the hippocampus proper, and then dropped again in the stratum radiatum at P80–90. In the dentate gyrus and corpus callosum, co-expression of NG2 and S100 β was very low (3 %) and constant throughout development. Age-related differences were also observed with Ki-67, a proliferation marker. In NG2 glia of the CA1 region, its expression decreased from 16 % at P10–12 to 9 % (P25–35) and then 3 % (P80–90). Triple-stainings revealed that Ki-67 was also expressed in 2–3 % of NG2/S100 β -positive cells in the juvenile and mature stratum radiatum, indicating that the latter, in contrast to S100 β -positive astrocytes, still host proliferative potential. Taken together, we found significant differences in transcript and protein expression, electrophysiological properties and proliferative capacity of NG2 glia in the mouse forebrain, suggesting the co-existence of several subpopulations of NG2 glia. Our data thus support the idea of a substantial regional and developmental heterogeneity in this subtype of macroglia.

B. Moshrefi-Ravasdjani, P. Dublin and G. Seifert equally contributed to this study.

Electronic supplementary material The online version of this article (doi:10.1007/s00429-016-1249-2) contains supplementary material, which is available to authorized users.

✉ Christine R. Rose
rose@uni-duesseldorf.de

¹ Institute of Neurobiology, Heinrich Heine University Düsseldorf, 40225 Düsseldorf, Germany

² Institute of Cellular Neurosciences, Medical Faculty, University of Bonn, 53105 Bonn, Germany

Keywords S100 β · NG2 · Hippocampus · Corpus callosum · Developmental profile · Heterogeneity

Introduction

NG2 glia are macroglial cells that are characterized by expression of the surface chondroitin sulphate proteoglycan NG2 (Horner et al. 2002; Nishiyama et al. 1996, 1999). They represent 8 % of the macroglial cells in the white and 3 % in the gray matter in adult mouse brain (Dawson et al. 2003). NG2 glia were first described as oligodendrocyte

precursor cells (Levine et al. 2001; Levine and Stallcup 1987) and have later on also been termed polydendrocytes (Nishiyama et al. 2002a), synantocytes (Butt et al. 2005) or GluR cells (Wallraff et al. 2004).

NG2 glia display characteristic electrophysiological properties and membrane currents distinct from those of other macroglial cells. Initially, cells expressing such ‘complex’ current patterns were regarded as immature astrocytes (Bergles et al. 2010; Bordey and Sontheimer 1997; Kressin et al. 1995). Subsequent analyses of transgenic mice expressing EGFP under the control of the hGFAP promoter (Nolte et al. 2001) indicated, however, that complex cells in the hippocampus display functional properties clearly different from astrocytes (Matthias et al. 2003; Wallraff et al. 2004). Specifically, while showing hGFAP promoter activity, complex cells expressed functional AMPA receptors, lacked glutamate transporters and did not exhibit gap junction coupling. Based on these findings, they were termed “GluR cells” to emphasize their expression of glutamate receptors. *Bona fide* astrocytes, in contrast, were devoid of ionotropic glutamate receptors, but expressed glutamate transporters and gap junctional coupling, and were thus termed “GluT cells”, emphasizing glutamate transport as a major characteristic (Matthias et al. 2003; Wallraff et al. 2004). Later work then showed that the vast majority of complex cells are also positive for NG2, indicating that this population indeed largely overlaps with NG2 glia (Nishiyama et al. 2009). In addition to glutamate receptors, NG2 glia express a large variety of other neurotransmitter receptors (Lin and Bergles 2002), and even form synapses with neurons (Bergles et al. 2000; Jabs et al. 2005). Moreover, they are characterized by expression of platelet-derived growth factor receptor α (PDGFR α) (Nishiyama et al. 2009).

Apart from these seemingly common properties, there is accumulating evidence that subpopulations of NG2 glia exist in different brain regions and during different developmental stages (Dimou and Gallo 2015; Steinhäuser and Dietrich 2015). This heterogeneity includes the expression of proteins like *proteolipid protein* (PLP) (Mallon et al. 2002) and TOAD-64, a common marker for immature neurons (Belachew et al. 2003). Other studies have established that some NG2 glia express proteins usually regarded as classical markers for astrocytes such as glutamine synthetase (Deloulme et al. 2004; Hachem et al. 2005; Polito and Reynolds 2005). In addition, there is evidence for expression of S100 β in NG2 glia (Karram et al. 2008). S100 β belongs to the large S100 family of Ca²⁺ binding proteins (Donato et al. 2013) and is characteristic of mature astrocytes of the hippocampus (Steiner et al. 2004). The onset of S100 β expression correlates with the loss of neural stem cell potential of GFAP-positive astrocytes in subventricular zone (Raponi et al. 2007) and in the subgranular

zone of the dentate gyrus (Gebara et al. 2016; Seri et al. 2004). Results concerning S100 β expression in NG2 glia are, however, inconsistent. While some studies reported no co-expression of S100 β and NG2 (Nishiyama et al. 1996), others found an almost complete overlap (Deloulme et al. 2004). In addition to these two extremes, 10 % of YFP-positive cells in the cortex of PDGFR α -CreERT2 mice, that is 10 % of presumed NG2 glia, were found to be also S100 β -positive (Rivers et al. 2008). Finally, using mice, which expressed EYFP under control of all regulatory elements of the NG2 gene, Karram et al. (2008) observed a co-localization of EYFP with S100 β in 20 % of (NG2) cells in juvenile mice and of 31 % in adult mice.

Another established difference in NG2 glia properties is the proliferative capacity of white matter versus gray matter cells. While in the cortex roughly 90 % remain NG2 glia, in the corpus callosum almost 60 % of NG2 glia become oligodendrocytes (Dimou and Gallo 2015). Studies in which the proliferative marker Ki67 was employed, suggest that the proliferative capacity of NG2 glia is generally low. In the white matter of the cerebellum, immunoreactivity for Ki67 was below 10 % at P7 and basically absent in adults (Zonouzi et al. 2015). A comparably low proliferative capacity was reported in the murine optic nerve (Solga et al. 2014). However, much higher proliferation rates have been suggested by others (Kukley et al. 2008; Rivers et al. 2008).

The discrepancies between different reports described above most likely result from the use of different mouse models and it is thus still largely unclear, to which extent certain functional properties of NG2 glia overlap with expression of different glial genes and with their proliferative capacity. In the present study, we, therefore, provide a comparative analysis of the molecular and functional properties of NG2 glia of the forebrain of different wild type and transgenic mice. Combining electrophysiological, transcript and immunocytochemical techniques, we first addressed the question whether “complex cells” in wild type mice and NG2-EYFP-positive cells found in mice expressing EYFP under control of the NG2 gene, comprise the same cell population (here subsumed as NG2 glia). Focusing on the hippocampus and corpus callosum, we then investigated the regional and temporal expression profile of S100 β in NG2 glia as well as expression of Ki67, a marker for proliferative activity, utilizing immunohistochemical tools.

Materials and methods

All experiments were carried out in accordance with the institutional guidelines of the Heinrich Heine University Duesseldorf, the Rheinische Friedrich Wilhelms University

Bonn as well as the European Communities Council Directive (86/609/EEC).

Animals and tissue preparation

For electrophysiology and RT-PCR, juvenile (P9–12) and adult (P40–60) mice (*mus musculus*, C57BL6J) were used. These were compared with NG2-EYFP mice (Karram et al. 2008), in which NG2 protein encoding sequence was replaced by EYFP (enhanced yellow fluorescent protein), and with hGFAP-EGFP mice (Nolte et al. 2001) as well as C57BL6J wild type mice.

Mice were killed by exposition to 50 % CO₂/50 % O₂. After decapitation, coronal hippocampal slices (150–200 μm) were cut in ice-cold oxygenated solution consisting of (in mM) 150 NaCl, 5 KCl, 2 MgSO₄, 1 N-pyruvate, 10 glucose, 10 HEPES, pH 7.4. Slices were maintained in artificial cerebrospinal fluid (ACSF) containing (in mM) 126 NaCl, 26 NaHCO₃, 3 KCl, 2 CaCl₂, 2 MgSO₄, 1.25 NaH₂PO₄, 10 glucose, equilibrated to a pH of 7.4 with 95 % O₂ and 5 % CO₂ at room temperature.

For the study of NG2, S100β and Ki-67 immunoreactivity, tissue slices obtained from mice (Balb/c) of both genders at different postnatal stages (P10–12, P25–35 and P80–90, six mice per age group, six sections per mouse) were used. Heterozygous NG2-EYFP mice (Karram et al. 2008) were used as a positive control, and homozygous NG2-EYFP mice (NG2^{-/-}, complete knock-out for NG2) as a negative control for validation of the specificity of the antibody for NG2 (see also below). Animals were killed with a mixture of 60 % xylazine and 40 % ketamine by intraperitoneal injections (0.1 ml of mixture/10 mg body weight). Transcardial perfusion was performed with 30–50 ml ice-cold phosphate buffered saline (PBS) and 30 ml ice-cold 4 % paraformaldehyde (PFA). Consecutively, brains were removed and post-fixed in 4 % PFA at 4 °C for 24–48 h. Brains were embedded in 3 % agar and cut in coronal plane with a vibratome (HM650V, Thermo Fischer Scientific, Walldorf, Germany) to prepare 30 μm thin sections. Tissue sections were stored until use at 4 °C in multiwells containing PBS supplemented with sodium azide.

Patch-clamp recordings

Whole-cell recordings were obtained in acute slices at room temperature. Slices were transferred to a recording chamber which was constantly perfused with ACSF. Pipettes were fabricated from borosilicate capillaries (Hildenberg, Malsfeld, Germany) and their resistances ranged from 3 to 6 MΩ when filled with a solution containing (in mM) 130 KCl, 10 HEPES, 5 BAPTA, 3 Na₂-ATP, 2 MgCl₂, 0.5 CaCl₂, pH 7.3. Current signals were amplified (EPC9; HEKA Elektronik, Lambrecht, Germany), filtered at 10 kHz, sampled at 6 kHz

and 30 kHz, respectively, and monitored with TIDA software (HEKA). Capacitance and series resistance (R_S) were compensated to improve voltage-clamp control. In NG2-EYFP animals, cells with NG2 promoter activity in the CA1 stratum radiatum were selected based on their EYFP fluorescence. NG2 glia in C57BL6J mice were identified according to their morphological and electrophysiological properties as reported (Jabs et al. 2005). In hGFAP-EGFP animals, NG2 glia were identified based on their EGFP fluorescence and electrophysiological properties (Matthias et al. 2003). Visual control was achieved with a microscope (Axioskop; Zeiss, Oberkochen, Germany) equipped with a CCD infrared camera (PCO, Kehlheim, Germany) and a 60× LUMPlan FI/IR objective (Olympus, Hamburg, Germany).

Membrane resistance (R_M), membrane capacitance (C_M) and R_S were determined by stepping the membrane from the holding potential (−70 mV) to −60 mV for 50 ms and analyzing data with Igor Pro 5.0.2.0. software (WaveMetrics, Lake Oswego, USA). The rectification index (RI) was determined by comparing membrane conductances at +20 and −130 mV:

$$RI = \frac{I_{(+20 \text{ mV})}}{(+20 \text{ mV} - E_{\text{rev}})} \bigg/ \frac{I_{(-130 \text{ mV})}}{(-130 \text{ mV} - E_{\text{rev}})} \quad (1)$$

where I is the maximal current amplitude and E_{rev} the reversal potential.

To test for statistically significant differences, Chi-square, Student's t or F test followed by Tukey's post hoc test were performed. The level of significance was set at $p < 0.05$.

Single-cell reverse transcription-PCR

Cell harvesting and RT followed a strategy described previously (Seifert et al. 2009). Immediately after recording, cells were lifted above the slice and sucked into the pipette under visual control. The pipette content was expelled into a tube filled with 3 μl diethylpyrocarbonate (DEPC)-treated water (Life technologies, Darmstadt, Germany) by breaking the tip of the pipette. The tube was frozen in liquid nitrogen and stored at −80 °C. RT was performed in a final volume of approximately 10 μl, adding RT buffer (Life technologies), deoxyribonucleotide triphosphates (dNTPs; final concentration 4 × 250 μM; Life technologies), random hexanucleotide primers (50 μM; Roche, Mannheim, Germany), dithiothreitol (DTT; 10 mM; Life technologies), ribonuclease (RNase) inhibitor (20 U; Promega, Mannheim, Germany) and Super-scriptIII reverse transcriptase (100 U; Life technologies). Additionally, total RNA prepared from freshly isolated mouse brain in DEPC-water and pure DEPC-water were used as positive and negative controls, respectively.

Incubation of the probes at 37 °C for 1 h resulted in the synthesis of single-strand cDNA. Then, nested multiplex PCR was performed, using the products obtained after the

first reaction as a template for the second PCR. The first PCR was performed in a final volume of approximately 50 μ l by adding PCR buffer, dimethyl sulfoxide (DMSO; 5 %; Sigma-Aldrich), MgCl₂ (2.5 mM), betaine (1 mM; Sigma-Aldrich) and corresponding primers (200 nM for NG2, GFAP and CNPase; 100 nM for S100 β ; Eurogentec, Seraing, Belgium). After denaturation, 5 U *Taq* polymerase (Life technologies) was added. 45 cycles were performed. Denaturation occurred at 94 °C for 25 s, primer annealing at 51 °C, 2 min for the first 5 cycles and 45 s for the remaining cycles. Primer extension was performed at 72 °C for 25 s. An aliquot (2 μ l) of the products of the first PCR was used as template for the second PCR (35 cycles; annealing temperature at 54 °C) using nested primers. The other reaction conditions remained unchanged, but dNTPs (4 \times 50 μ M) and 2.5 U Platinum *Taq* polymerase (Life technologies) were added. Products were identified by agarose gel electrophoresis (1.5 %; stained with ethidium bromide) using a molecular weight marker (Φ X-174 *HincII* digest; Eurogentec). Table 1 gives an overview of the primers used for the PCRs and the length of the amplified products.

Immunohistochemistry

For epifluorescence analysis, indirect immunohistochemical staining was executed at free-floating sections in multiwell plates. Sections were blocked and permeabilized at room temperature, using a blocking solution consisting of 5 % normal goat serum (NGS; GIBCO/Life Technologies, Darmstadt, Germany) and 0.4 % TritonX-

100 (Sigma-Aldrich Chemical, Munich, Germany) resolved in PBS. Afterwards, samples were incubated in blocking solution containing primary antibodies [rabbit anti-NG2 (1:250, Millipore, Billerica, MA, USA), mouse anti-S100 β (1:1000, Abcam, Cambridge, UK), rabbit anti-Ki-67 (1:250, Abcam, Cambridge, UK) or chicken anti-GFP (1:1000, Abcam, Cambridge, UK)] at 4 °C overnight. Sections were then washed with blocking solution 3 \times 20 min. The following steps were performed at room temperature and in the dark. Tissue sections were incubated with secondary antibodies (goat anti-mouse, chicken and rabbit (1:500, Invitrogen, Grand Island, NY, USA) conjugated with Alexa Fluor488, Alexa Fluor594 or Alexa Fluor633. Secondary antibodies were diluted in PBS with 2 % NGS. After incubation for 90 min, sections were washed with PBS 3 \times 5 min. DAPI was added to the wells for 20 min to receive nuclear stainings. Afterwards, the sections were washed with PBS for 3 \times 5 min, mounted on microscope slides and coverslipped with Mowiol (Calbiochem, Fluka, distributed by Sigma-Aldrich Chemical, Munich, Germany) or Mountant Permafluor (Thermo Fisher Scientific, Schwerte, Germany).

To verify the specificity of the antibody against NG2, tissue sections from NG2^{-/-} animals (Karram et al. 2008) were immunohistochemically labelled for NG2 and compared with tissue from their heterozygous littermates (three mice per genotype, four sections per mouse). Labelling for NG2 in hippocampal tissue derived from NG2^{-/-} mice animals resulted in weak non-specific background signals

Table 1 Primers for RT-PCR

Gene	Sequence	Position	Product length (bp)	Accession no.
S100 β	se 5'-aggccatggtgccctcattgat	17	246	NM_009115
	as 5'-ACTCATGGCAGGCCGTGGTCA	242		
S100 β (nested)	se 5'-tactccggcgagagggtgaaa	52	186	
	as 5'-GGCGACGAAGGCCATGAACTCC	216		
NG2	se 5'-cacactctctctggacatttcttc	4708	358	NM_139001
	as 5'-TGGCAGGTGGTGAGGACAGT	5046		
NG2 (nested)	se 5'-ggaggcaccgggaagtga	4767	155	
	as 5'-GCTGGGCATGGAGGAGTCG	4903		
CNP 1	se 5'-gcccgggctggagaaggact	471	408	NM_001146318
	as 5'-AGATCACTGGGCCACAACCTGC	858		
CNP 1 (nested)	se 5'-actctactttggctggtctctgac	498	256	
	as 5'-CTCCTGCTGGGCGTATTCTTCTGC	730		
GFAP β	se 5'-GctccccaagccaaGcacgaa	809	435	NM_010277
	as 5'-TCACCATCCCGCATCTCCACAGTC	1220		
GFAP β (nested)	se 5'-cgccaactcgagccttgacct	850	350	
	as 5'-TGGCCTTCTGACACGGATTTGGTG	1176		

'Se' and 'as' mark sense and antisense primers. Position 1 is the first nucleotide of the initiation codon. All sense and antisense primers are located on different exons, respectively

similar to what was found in the negative control labels (data not shown). In the NG2-EYFP heterozygous littermates, in contrast, high intensity signal levels with co-localisation degree of 97 % were obtained for the NG2 antibody (data not shown). These results demonstrate that labelling for NG2 was highly specific in the murine brain. Identical conditions in tissue processing were employed in all individually performed stainings. Negative controls were run in parallel to each staining by either omitting all or one of the primary antibodies. Omitting one of the primary antibodies exhibited identical labeling patterns for the remaining antibody as for the double stainings. Excluding both primary antibodies never resulted in a specific staining.

For triple stainings involving anti-NG2, anti-S100 β and anti-Ki-67, NG2 antibody (1:125) was conjugated with a fluorescent dye provided by an antibody labeling kit (Life Technologies, Grand Island, NY, USA). Tissue sections were first stained for S100 β and Ki-67 as described above. Then, sections were incubated with NG2 antibody only in blocking solution for 24 h. Finally the antibody was washed out, and the staining procedure was continued as described above.

Documentation and analysis of immunofluorescence

Widefield epifluorescence images were acquired at a Nikon Eclipse 90i microscope (Nikon Instruments, Düsseldorf, Germany). The microscope was equipped with standard DAPI (EX 340–380; DM 400; BA 435–485), FITC (EX 465–495; DM 505; BA 515–555), and TRITC (EX 540/25; DM 365; BA 605/55) filter sets. Illumination was provided by an Intensi-light fiber lamp (C-GHFI; Nikon Instruments, Düsseldorf, Germany), and emission was detected with a monochrome digital camera (DS-Qi1Mc; Nikon Instruments, Düsseldorf, Germany). Coronal z-stacks with ten to twenty 1 μ m or 1.8 μ m steps were captured with a planapochromat Nikon 20 \times /0.75 objective. NIS-Elements software (Nikon Instruments, Düsseldorf, Germany) was used for image acquisition. Simultaneous or sequential imaging of both fluorophores revealed no difference in their staining pattern, indicating no cross-excitation or spectral bleed-through. Alternatively, confocal z-stacks (10–20 optical sections, 0.3–0.5 μ m each) were captured with an upright confocal laser scanning microscope (Nikon C1 Nikon with Eclipse E600FN and a Nikon 60 \times /1.4 oil objective; Nikon Instruments, Düsseldorf, Germany).

Image stacks were captured in the hippocampal CA1 regions stratum radiatum and stratum oriens, in the dentate gyrus and the corpus callosum. PMT settings and image processing were kept constant when comparing the different age groups. Simultaneous or sequential scanning of both fluorophores revealed no difference in their staining

patterns, indicating no cross-excitation or spectral bleed-through. Images were edited with ImageJ (NIH Image, Bethesda, MD, USA), including background correction, color balance and contrast and insertion of scale bars. Adobe Illustrator CS2 (Adobe Systems Incorporated, San Jose, CA, USA) was used for image presentation.

ImageJ plugin CellCounter was used to count cells to define the level of co-expression. Mean values and standard errors of the mean (SEM) were calculated in Excel (Microsoft Office Excel 2010, SSL, Redmond, WA, USA). To assess significance in differences between groups, Chi-square, Wilcoxon-Mann-Whitney and Fisher exact tests were applied using Gnumeric 1.12 (The GNOME Project) and QuickCalcs (GraphPad Software, Inc) with $p \leq 0.05$ (*) and $p \leq 0.01$ being significant (**). Graphs were made in Excel and edited in Adobe Illustrator CS2.

Results

In the present study, we combined electrophysiological, transcript and immunocytochemical analyses to reveal the regional and temporal heterogeneity of NG2 glia in the mouse hippocampus, dentate gyrus and corpus callosum.

Functional properties of NG2 glia

In the first set of experiments, we compared the electrophysiological properties of NG2 glia located in the CA1 stratum radiatum in C57BL6J mice with those of NG2-EYFP-positive cells found in mice expressing EYFP in place of the NG2 gene (Karram et al. 2008). In addition, NG2 glia, selected based on their EGFP fluorescence and electrophysiological characteristics, were studied in hGFAP-EGFP mice. To reveal changes during postnatal development of the hippocampus, both juvenile and adult animals were analyzed (C57BL6J: $n = 5$ juvenile and $n = 6$ adult mice; NG2/EYFP: $n = 7$ juvenile and $n = 4$ adult mice; hGFAP-EGFP: $n = 30$ juvenile and $n = 18$ adult mice; Tables 2, 3).

All cells analyzed displayed a ‘complex’ whole-cell current pattern composed of voltage- and time-dependent outward currents and inwardly rectifying currents as reported previously (Fig. 1a, b) (Karram et al. 2008; Matthias et al. 2003; Steinhäuser et al. 1994). In juvenile mice, resting potential, membrane resistance, membrane capacitance, current density at -130 mV and the rectification index of membrane conductances determined at $+20$ and -130 mV did not show significant differences between genotypes (Table 2). Comparison of cells from juvenile and adult mice within the same genotype revealed a developmental increase of expression of inwardly rectifying K^+ (Kir) channels, resulting in a higher current density

Table 2 Passive membrane properties of NG2 cells in the CA1 stratum radiatum of juvenile NG2-EYFP, C57BL6J and hGFAP-EGFP mice

Genotype	<i>n</i>	V_r (mV)	R_m (M Ω)	C_m (pF)	CD _{-130 mV} (pA/pF)	RI (g _{20 mV/g} -130 mV)
NG2-EYFP	47	-74.5 ± 14.5	487.8 ± 568.0	29.0 ± 10.6	-10.5 ± 4.3	6.3 ± 3.8
C57BL6J	21	-80.9 ± 7.0	744.5 ± 1350.7	36.5 ± 17.5	-9.7 ± 4.3	6.4 ± 5.1
hGFAP-EGFP	30	-79.2 ± 13.9	427.5 ± 323.4	27.6 ± 12.9	-9.9 ± 3.6	5.6 ± 3.4

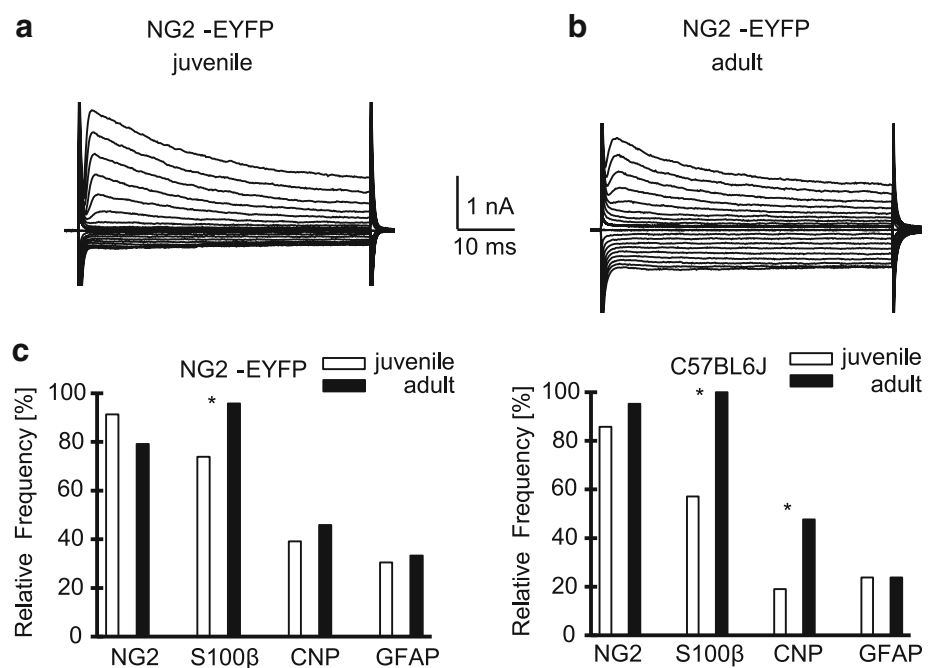
Recordings of NG2 glia were obtained in situ from p9–p12 old mice. Responses were activated by de- and hyperpolarization of the cell membrane between -160 and +20 mV (10 mV increments; holding potential -70 mV). Resting potential (V_r), membrane resistance (R_m), membrane capacitance (C_m), current density at -130 mV (CD_{-130mV}) and rectification index (RI) were compared

Table 3 Passive membrane properties of NG2 cells in the CA1 stratum radiatum of adult NG2-EYFP, C57BL6J and hGFAP-EGFP mice

Genotype	<i>n</i>	V_r (mV)	R_m (M Ω)	C_m (pF)	CD _{-130 mV} (pA/pF)	RI (g _{20 mV/g} -130 mV)
NG2-EYFP	23	-80.3 ± 8.0	139.1 ± 78.1	25.7 ± 7.3*	-17.6 ± 4.5	1.9 ± 0.7
C57BL6J	18	-82.4 ± 8.7	200.8 ± 122.2*	25.5 ± 7.4	-15.8 ± 4.4	2.3 ± 0.8
hGFAP-EGFP	18	-77.1 ± 8.3	107.5 ± 45.7*	30.8 ± 5.2*	-18.6 ± 5.4	1.9 ± 0.5

Recordings of NG2 glia were obtained in situ from p40–p60 old mice. Responses were activated as described above. Asterisks denote significant differences between genotypes ($p < 0.05$)

Fig. 1 Heterogeneous profiles of mRNA encoding NG2, S100 β , CNP and GFAP in NG2 glia from different mouse strains. **a, b** Current pattern of NG2 glia in situ from NG2-EYFP mice (heterozygous) after de- and hyperpolarization of the membrane between -160 and +20 mV (10 mV increments; holding potential was -70 mV). The cells at P10 (**a**) and P48 (**b**) had resting potentials of -89 and -86 mV, respectively. After harvesting of cytoplasm and RT-PCR, expression of NG2 and S100 β mRNA was detected. **c** Summary of the relative frequency of transcript expression. Asterisks mark significant differences between juvenile and adult mice



at -130 mV, a lower rectification index and lower membrane resistance. In C57BL6J mice, the membrane capacitance of NG2 glia in older mice was lower than in cells from juvenile mice (Table 3).

In summary, these data demonstrate that the passive membrane properties and voltage-dependent ion currents of “complex cells”, NG2-EYFP cells and “GluR cells” as identified in the different mouse strains are essentially undistinguishable at P9–12. In addition, we found a similar developmental increase in functional Kir channel

expression in the three genotypes analysed. The largely identical electrophysiological properties suggest that the foresaid cells belong to the same cell population, from now on named NG2 glia.

Single-cell transcript expression patterns of NG2 glia

To compare the gene expression profiles of NG2 glia from different mouse strains subsequent to electrophysiological

analysis, we performed single cell RT-PCRs with primers for NG2, GFAP, S100 β and CNP1 mRNA. In contrast to the similarity in their electrophysiological properties, NG2 glia from juvenile NG2-EYFP ($n = 23$ cells) and C57BL6J mice ($n = 21$) (suppl. Figure 1) displayed distinct expression profiles for the analysed genes. The most frequent gene transcript combination in cells from NG2-EYFP mice was co-expression of NG2 and S100 β mRNA. By contrast, cells from juvenile C57BL6J mice mostly expressed only NG2 transcripts. Next we compared the expression profile of NG2 glia in adult NG2-EYFP ($n = 24$) and C57BL6J mice ($n = 21$). Co-expression of NG2 and S100 β mRNA occurred most frequently in the two mouse lines (Fig. 1c). When comparing the relative frequencies of gene expression in cells from juvenile versus adult mice within a given strain, no significant difference was observed. Comparison of developmental changes in gene expression within the respective mouse strains revealed an increase of S100 β mRNA frequency in NG2 glia of NG2-EYFP and C57BL6J mice, and an increase of CNP expression in C57BL6J mice (Fig. 1c).

Interestingly, while the functional properties of NG2 glia largely overlapped, single-cell mRNA expression of glial genes thus displayed distinct differences between different mouse strains.

Spatial and temporal characteristics of NG2 protein expression

To study NG2 expression at the protein level and reveal its cellular and regional distribution, immunohistochemistry was employed. To this end, three stages of postnatal development were analysed: P10–12 (juvenile), P25–35 (young adult), and P80–90 (adult). The pattern of NG2 immunoreactivity was studied in the hippocampal CA1 region, the hilus of the dentate gyrus and in the corpus callosum.

NG2 glia appeared to be densely packed in all regions of juvenile mice (P10–12) but seemed highest in the corpus callosum, followed by the CA1 region and lowest in the hilus. In the CA1 region and the corpus callosum, the immunoreactivity decreased drastically to P25–35 and again towards adulthood (P80–90) (Fig. 2a). In the hilus, in contrast, the degree of immunoreactivity remained at comparable low levels until adulthood. While the cell density decreased in the CA1 region, the domains of single NG2-positive cells increased towards adulthood (Fig. 2a insets). Quantitative analyses of the cell densities revealed that in the two grey matter CA1 regions stratum radiatum and stratum oriens, the number of NG2-positive glia per

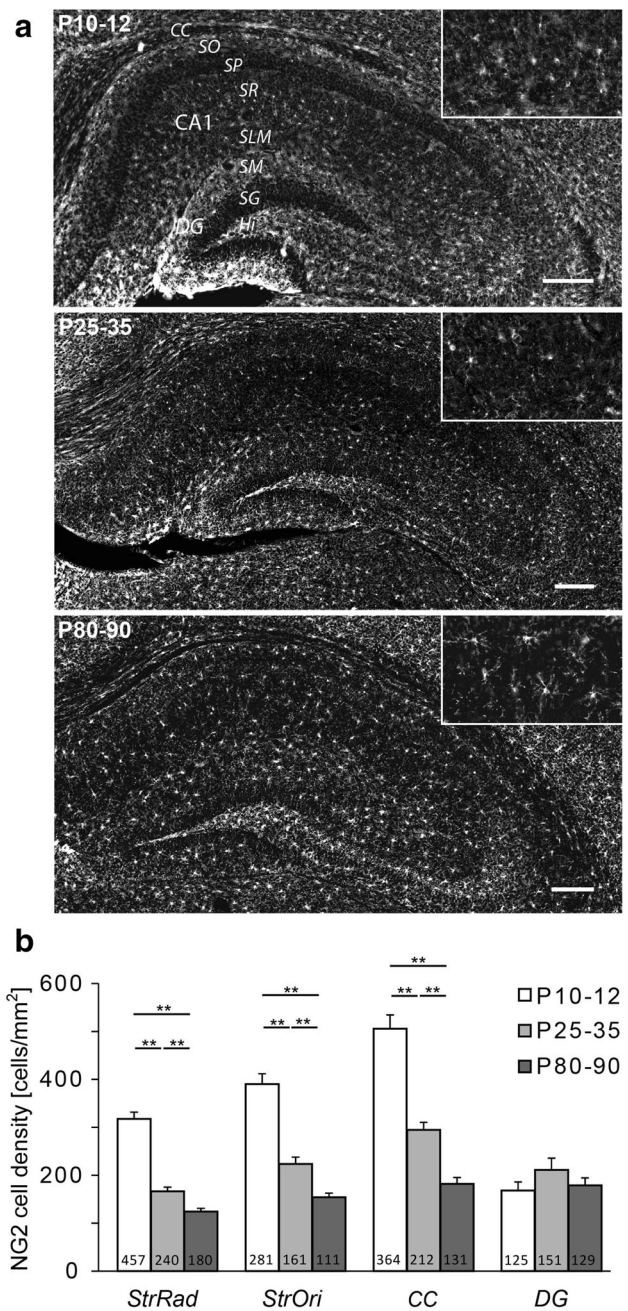


Fig. 2 Spatio-temporal distribution of NG2 glia in the hippocampal formation. **a** Stitches of images taken in the hippocampal formation of mice of different age groups (P10–12; P25–35; P80–90) revealed a decrease in NG2-immunoreactive cell density in ageing mice. The insets show close-ups of the CA1 str. radiatum. Scale bars 100 μ m. **b** Bar chart showing the density of NG2-positive cells. A decrease in the density of NG2-positive cells was found in the CA1 region and corpus callosum of older mice but not the hilus of the dentate gyrus. Numbers in bars represent the total number of cells counted per age group CA1 Cornu ammonis 1, CC corpus callosum, SO stratum oriens, SP stratum pyramidale, SR stratum radiatum, SLM stratum lacunosum moleculare, SM stratum moleculare, SG stratum granulosum, Hi hilus, DG dentate gyrus

mm² was highest at P10–12 with 317.4 ± 14.3 cells/mm² (str. radiatum) and 390.3 ± 21.4 cells/mm² (str. oriens) (Fig. 2b). At P25–35, the cell density was significantly decreased to 166.7 ± 8.6 and 223.6 ± 14.2 cells/mm², respectively. At P80–90, finally, these numbers were further significantly reduced to 124.3 ± 6.9 cells/mm² (str. radiatum) and 154.2 ± 8.4 cells/mm² (str. oriens) (Fig. 2b). Thus, in these hippocampal gray matter regions the density of NG2 cells decreased by roughly a factor of 2. Taking into account that the volume of the hippocampus approximately doubles during the same period (Zhang et al. 2005) the overall number of cells thus almost remained constant in the stratum radiatum and the stratum oriens from P10–12 on.

In the corpus callosum of older animals, a highly myelinated white matter region, the initial cell density was even higher with 505.6 ± 28.9 cells/mm². Here, the density declined significantly to 294.4 ± 16.2 cells/mm² at P25–35 and to 181.9 ± 13.3 cells/mm² at P80–90 (Fig. 2b). In contrast, an age-dependent decrease in NG2 cell density was not observed in the hilus of the dentate gyrus, where numbers varied only slightly, ranging from 173.6 ± 21.4 cells/mm² at P10–12 to 205.6 ± 14.8 cells/mm² at P25–35 and 179.2 ± 14.8 cells/mm² in the oldest age group (Fig. 2b).

Taken together, our stainings revealed a strong decrease in the density (but not the overall number) of NG2 expressing cells in the stratum radiatum, stratum oriens and corpus callosum from juvenile to adult animals. In contrast, NG2 expression remained at a constant low level in the dentate gyrus throughout all developmental stages.

Temporal and spatial heterogeneity of NG2/S100 β co-localization

Our single cell RT-PCR analysis revealed a strong overlap of NG2 and S100 β mRNA expression in NG2-EYFP mice. To study the regional and temporal expression profile of S100 β in NG2 glia at the protein level, we immunohistochemically co-labelled both proteins. Our stainings revealed co-localization of NG2/S100 β in 2–27 % of cells, depending on the brain region and developmental stage (Figs. 3, 4, 5, 6). High magnification confocal images served to clarify the subcellular location of both proteins (Fig. 3c). While NG2 was mostly located at the plasma membrane, S100 β was usually seen in the cytosol. Overlap of fluorescence was thus mainly found in primary processes and at the soma membrane (Fig. 3c).

Cells immunoreactive for both NG2 and S100 β were largely restricted to the CA1 areas of all ages (Fig. 3a), while in the corpus callosum and the dentate gyrus (Figs. 4, 5), NG2/S100 β co-localization occurred only sparsely. Quantitative analyses of the degree of co-expression in the

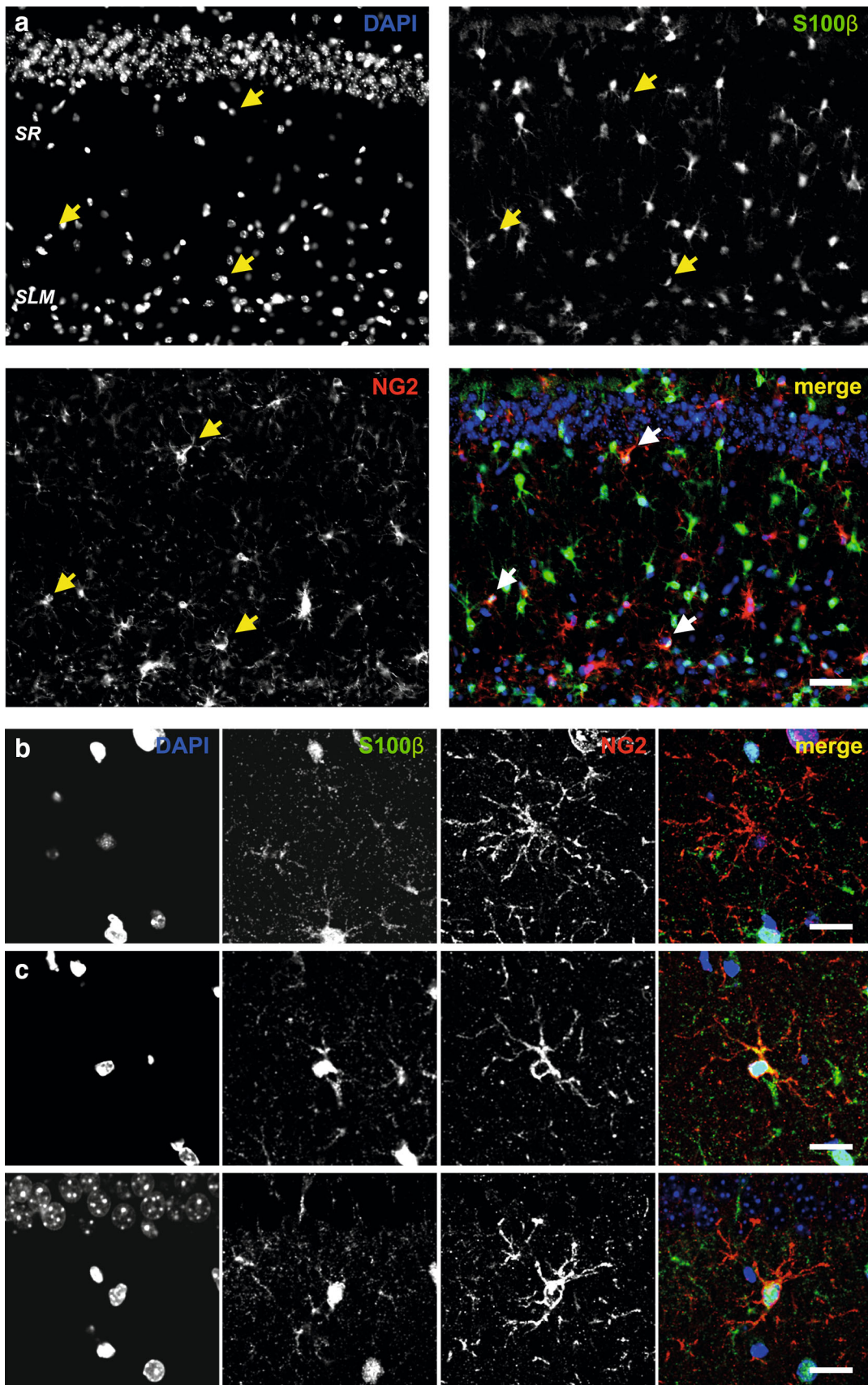
Fig. 3 Co-localization of NG2 and S100 β immunoreactivity in the murine hippocampus. **a** Epifluorescence images of a triple labeling for S100 β (green), NG2 (red) and DAPI (blue) in the hippocampus of a P32 mouse. A subset of NG2-positive cells was also immunoreactive for S100 β (arrows). DAPI is shown in blue. SR stratum radiatum, SLM stratum lacunosum moleculare. Scale bar 40 μ m. **b** Confocal images of a CA1 NG2 cell. The expression of membrane-associated NG2 (red) and the location of cell nuclei (blue) are displayed. Scale bar 20 μ m. **c** Confocal images of a CA1 NG2 cell co-immunoreactive for S100 β . The co-expression of cytosolic S100 β (green), membrane-associated NG2 (red) and the location of cell nuclei (blue) is displayed. Scale bar 20 μ m

abovementioned regions and age groups revealed co-expression of 7.2 ± 1.2 % ($n = 457$) in the stratum radiatum of P10–12 animals (Fig. 6). The percentage of double-labelled cells in this sub-region significantly increased to 26.9 ± 2.8 % ($n = 240$) at P25–35 and significantly decreased thereafter to 13.7 ± 2.8 % ($n = 180$) in adult animals (Fig. 6). In the stratum oriens, NG2/S100 β -expressing cells constituted 3.8 ± 1.4 % of all NG2 glia ($n = 281$) in juvenile mice (Figs. 4, 6). Their relative number increased to 14.4 ± 3.6 % ($n = 161$) at P25–35 and to 12.1 ± 3.7 % ($n = 111$) at P80–90 (Figs. 4, 6). Co-localization in the corpus callosum remained at constant low levels throughout development (1 ± 0.6 % ($n = 364$) at P10–12; 1.5 ± 0.7 % ($n = 212$) at P25–35; 2.7 ± 1.3 % ($n = 131$) at P80–90; Figs. 4, 6). In the dentate gyrus, NG2-positive cells expressed S100 β to a similar degree (P10–12: 2.5 ± 1.4 %, $n = 125$; Fig. 5). No significant differences were found between different groups (P25–35: 5.4 ± 1.8 %, $n = 151$; P80–90: 9.4 ± 2.3 %, $n = 129$; Fig. 6).

In summary, we found clear evidence that a subset of NG2 glia also expresses S100 β at the protein level. Expression is, however, strongly dependent on the brain region and developmental stage. Immunoreactivity patterns of S100 β expression in NG2-positive cells of the hippocampal CA1 regions stratum radiatum and stratum oriens were strongest at P25–35. In contrast, NG2 glia of the corpus callosum and dentate gyrus displayed low co-expression levels of S100 β that remained relatively constant during postnatal development.

Proliferative potential of NG2/S100 β -positive cells

Our results obtained so far indicated that a subset of NG2 glia also expresses S100 β . Because the latter is commonly used as a marker for mature (non-proliferative) astrocytes, we addressed the question if expression of S100 β in NG2 glia at the different postnatal stages of development is correlated with a general loss of their proliferation capacity. To this end, immunohistochemistry for Ki67, a



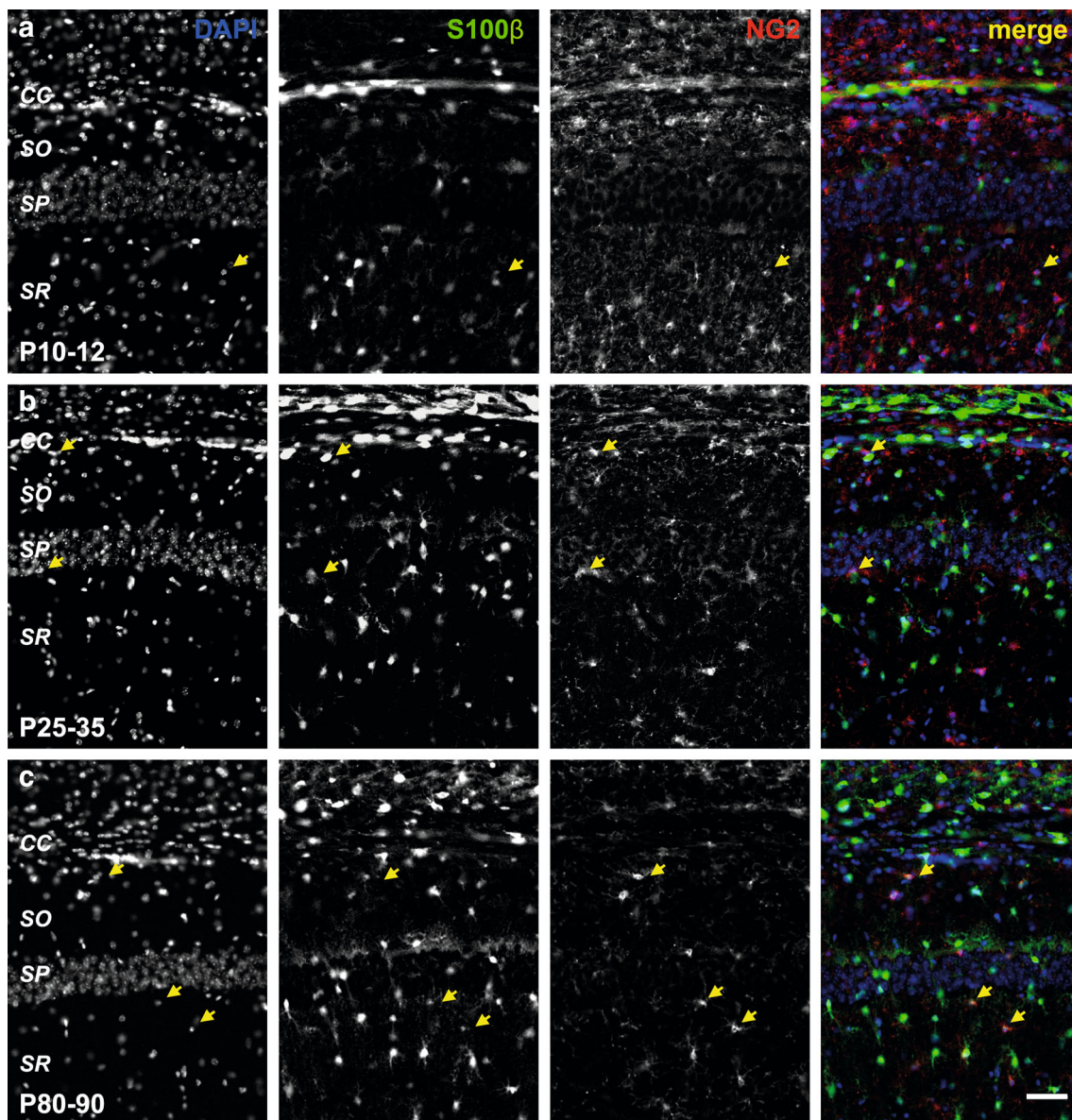


Fig. 4 Developmental profile of the immunoreactivity for S100 β and membrane-associated NG2 in the mouse hippocampal CA1 region and corpus callosum. The expression of cytosolic S100 β (green), membrane associated NG2 (red) and location of cell nuclei (blue) is

displayed in mice at **a** P10–12, **b** P25–35, and **c** P80–90. Arrows point to double-positive cells. CC corpus callosum, SO stratum oriens, SP stratum pyramidale, SR stratum radiatum. Scale bar 40 μ m

proliferation marker was performed. Expression levels of Ki-67 were analyzed both in cells positive for NG2 and S100 β as well as in NG2-positive/S100 β -negative cells to gain insight into possible differences in the proliferation capacity between these two groups.

Triple-staining for NG2, S100 β and Ki-67 indicated that proliferation of NG2 glia is higher in juvenile mice (Fig. 7). S100 β -negative/NG2-positive cells displayed a significant decrease in the Ki-67 expression with age from 15.8 ± 2.1 % ($n = 213$) in P10–12 to 8.6 ± 2.5 % ($n = 187$) in P25–35 and to 3 ± 1.4 % ($n = 141$) in

P80–90 (Fig. 8). In contrast, S100 β -positive NG2 glia never co-expressed Ki67 at P10–12 and at later stages, only low levels of Ki67 immunoreactivity were found (P25–35: 2.5 ± 1.7 %, $n = 187$; P80–90: 2.8 ± 2.7 %, $n = 141$; Figs. 7, 8). We never detected Ki-67 expression in NG2-negative but S100 β -positive cells. An example of a cell in the stratum radiatum which was positive for all three antigens is shown in Fig. 8b.

This set of experiments thus indicated that S100 β -negative NG2 glia in juvenile animals host a significant proliferative potential that decreases upon maturation in the

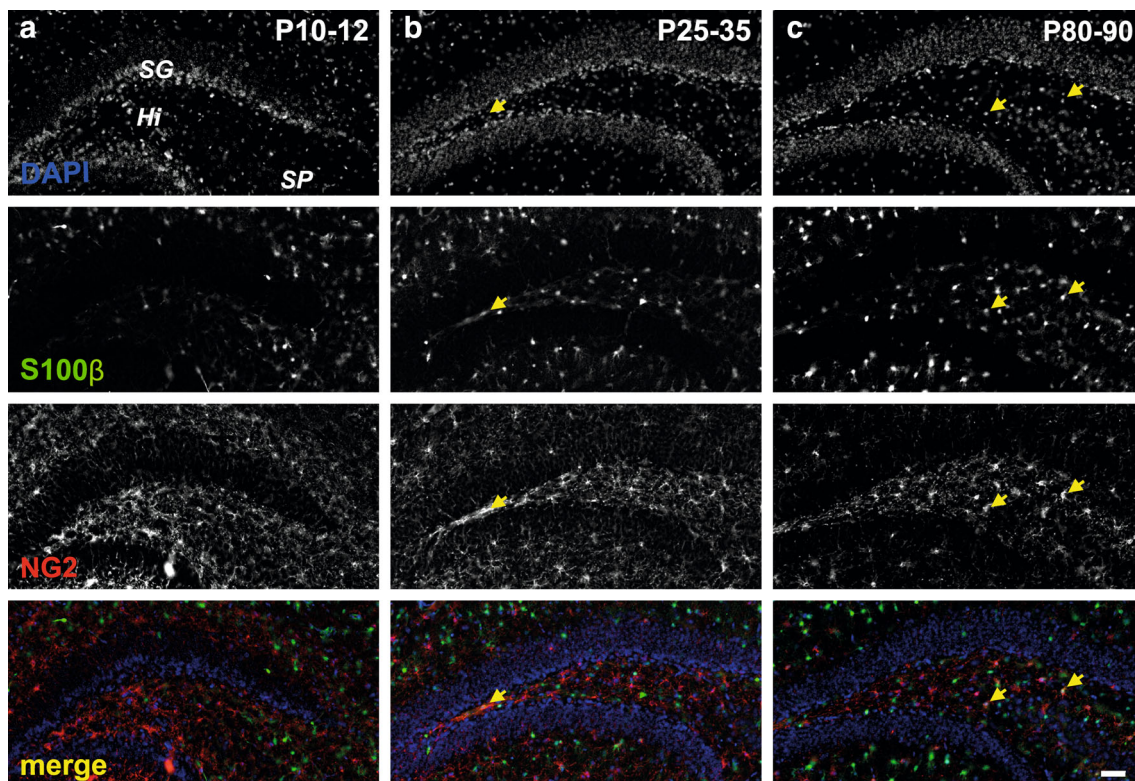


Fig. 5 Developmental profile of the immunoreactivity for S100 β and membrane-associated NG2 in the *hilus* of the mouse dentate gyrus. The expression of cytosolic S100 β (*green*), membrane associated NG2 (*red*) and location of cell nuclei (*blue*) is displayed in mice at

a P10–12, **b** P25–35, and **c** P80–90. *Arrows* point out double-positive cells. *SG* stratum granulosum, *Hi* hilus, *SP* stratum pyramidale. *Scale bar* 50 μ m

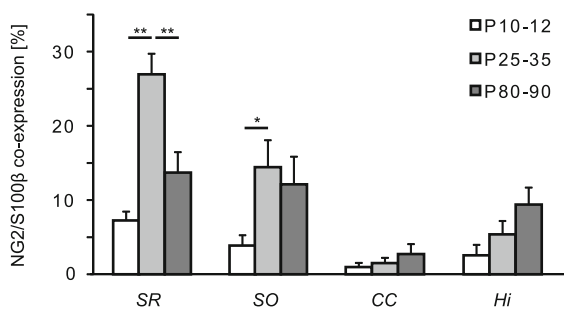


Fig. 6 Quantification of NG2/S100 β co-expression. Spatial and temporal heterogeneity of S100 β expression in NG2 glia. In the stratum radiatum and stratum oriens, significant changes in co-expression were observed upon ageing, while the corpus callosum and hilus of the dentate gyrus did not feature significant changes. *SR* stratum radiatum, *SO* stratum oriens, *CC* corpus callosum, *Hi* hilus

hippocampal CA1 region. In contrast, juvenile S100 β -positive NG2 glia never showed labeling for Ki-67. Taken together, our data thus suggest that expression of S100 β in NG2 glia in juvenile to adult brains goes along with a significant reduction in their proliferative activity. Accordingly, expression of S100 β characterizes a population of NG2 glia with no (P10–12) or low (P25–35 and adult) proliferative potential.

Discussion

In the present study, we analyzed the molecular and functional properties of NG2 glia of the forebrain of different mouse strains, employing electrophysiological, molecular biological, and immunohistochemical tools. The main focus was on the investigation of the regional and temporal expression profile of S100 β in NG2 glia as well as on their proliferative capacity.

Passive membrane properties and inward currents in NG2 glia

Irrespective of the age of the transgenic mice, all NG2 glial cells displayed a ‘complex’ current pattern consisting of voltage- and time-dependent in- and outward currents. In juvenile mice, Kir current densities and rectification index were highly variable, but on average significantly lower than in adult mice. These data confirm earlier findings obtained from ‘complex glial cells’ in C57BL6 (Kressin et al. 1995) and NG2-YFP mice (Passlick et al. 2016). Only grey matter NG2 glia have already a pronounced Kir current density at the juvenile stage, producing lower resting potentials and input resistance as compared to white matter

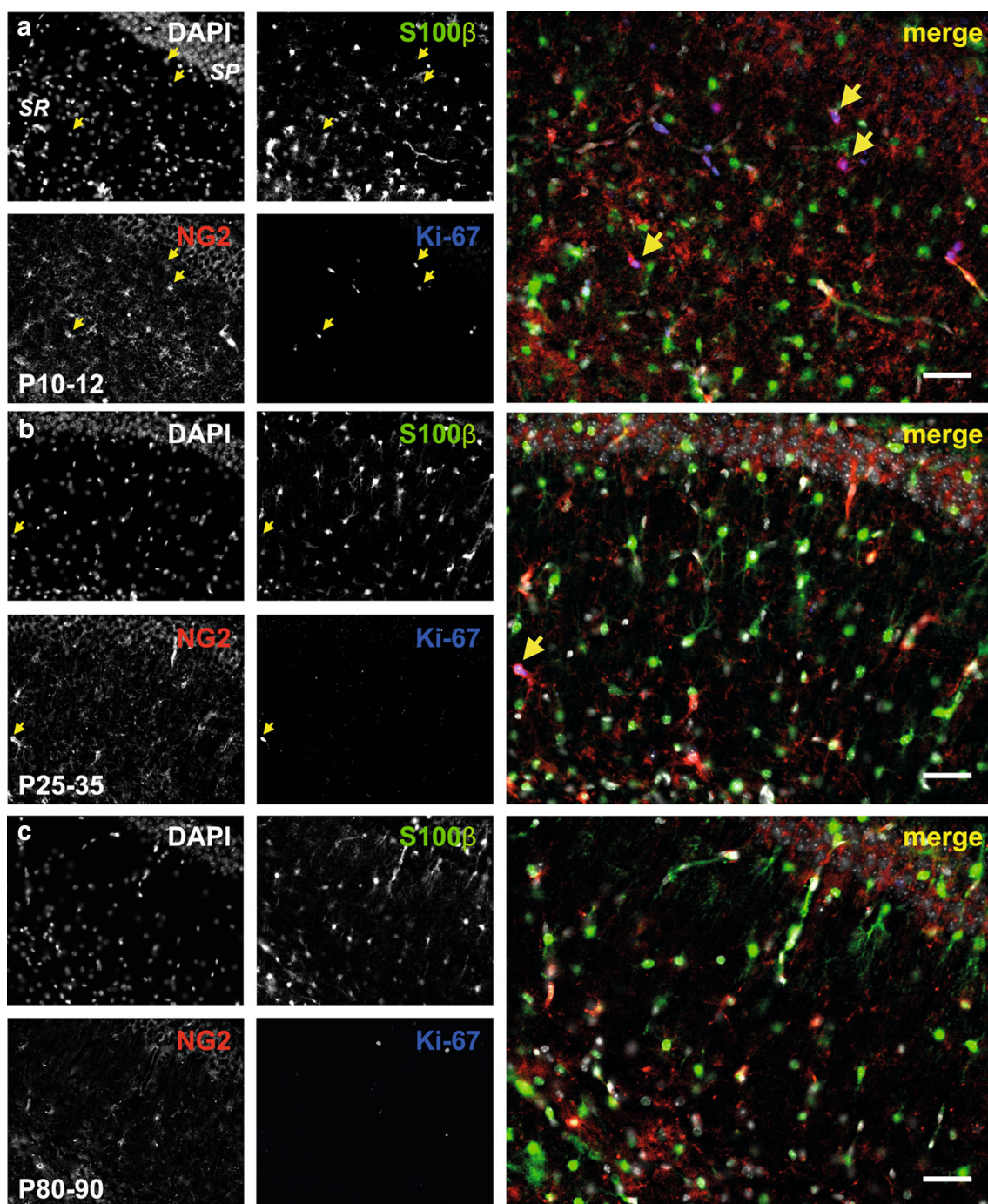


Fig. 7 Developmental profile of the immunoreactivity for Ki67 in S100 β -negative NG2 glia in the mouse hippocampal CA1 region. Immunohistochemical triple staining targeting NG2 (red), S100 β (green) and the proliferation marker Ki67 (blue). DAPI is shown in addition solely as gray scale image in the merges. Among all age

groups (**a** P10–12, **b** P25–35, **c** P80–90) a small subset of S100 β -negative NG2-positive cells expresses of Ki67 (arrows), which decreases upon ageing. SP stratum pyramidale, SR stratum radiatum. Scale bar 40 μ m

NG2 glia (Chittajallu et al. 2004). These channels detect local changes of extracellular K⁺ during neuronal activity and are composed of the Kir4.1 subunit (Djukic et al. 2007; Maldonado et al. 2013; Schröder et al. 2002). The variable

expression of Kir currents in juvenile hippocampus might be due to different developmental stages of the NG2 glia because during maturation current densities increased and became more homogeneous.

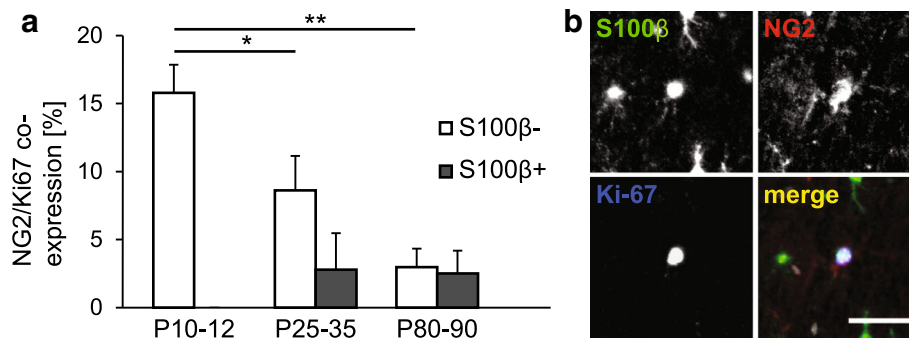


Fig. 8 Quantification of Ki67-, S100 β -, and NG2-immunoreactivity in the mouse hippocampal CA1 region. **a** Bar chart showing the quantification of NG2+/Ki67+/S100 β + cells and NG2+/Ki67+/S100 β - cells during development. At P25–35 and P80–90 a low number of NG2/S100 β co-expressing cells were additionally positive

for Ki67. But note that the NG2+/Ki67+/S100 β - cells were already present at P10–12 and the number decreased over development. **b** Representative immunophotomicrograph showing a NG2 glial cell in the str. radiatum that features an intensive cytosolic S100 β staining and is Ki67-positive. Scale bar 40 μ m

Gene expression profile of NG2 glia

Previous work has already demonstrated that some NG2 glia display GFAP or CNP promoter activity and immunoreactivity for S100 β , i.e. share these properties with astrocytes and oligodendrocytes (Jabs et al. 2005; Matthias et al. 2003; Yuan et al. 2002). However, it was unclear whether all NG2 glial cells exhibit these properties or whether these cells are heterogeneous with regard to their expression profiles. Our single cell RT-PCR analyses clearly demonstrated that the different glial genes are expressed at a variable extent across NG2 glia, independent of developmental stage and genetic background. While the majority of cells expressed mRNA for NG2 and S100 β (Haberlandt et al. 2011), the expression frequencies of transcripts encoding GFAP or CNP were significantly lower. Notably, the presence of mRNA for GFAP and CNP in some cells and the abundant expression of S100 β transcripts differed from the cells' immunocytochemical properties because under physiological conditions NG2 glia do not express GFAP or CNP on a protein level, and S100 β is found only in a minority of cells (Karram et al. 2008; Yuan et al. 2002) (Fig. 1, suppl. Figure 1 in the present study). However, the transcript data give a clue to understand why these cells can differentiate into astrocytes or oligodendrocytes under pathological conditions (Dimou and Gallo 2015).

Spatial and temporal profile of NG2 protein expression

Our work shows that the expression pattern of NG2, i.e. the number and density of NG2 glia strongly depends on the brain region and developmental stage investigated. To determine the number and distribution of NG2 glia, we employed immunohistochemistry against NG2. NG2,

however, has been shown to undergo cleavage of its ectodomain which is then deposited at the extracellular matrix (Asher et al. 2005). To avoid this potential problem of false-positive labeling, we analyzed only cells with a clear NG2 glial morphology: For example, an elongated (in the white matter) or round (in the gray matter) cell body and numerous thin processes exhibiting a seemingly constant diameter along their entire length (Berry et al. 2002; Chen et al. 2008). To avoid that a potential low specificity of the NG2 antibody used might affect labelling intensity and the analysis of the cell densities, we additionally examined the antibody specificity by determining the co-expression of NG2 and EYFP in NG2 glial cells utilizing NG2-EYFP mice (Karram et al. 2008). Analysis of NG2-EYFP heterozygous mice revealed a degree of co-expression of 97%. In tissue sections from NG2-EYFP homozygous mice (which are completely lacking NG2), we observed no specific staining of NG2, confirming a high specificity of the applied antibody.

Having demonstrated the antibody's specificity, the general expression pattern of NG2 and the spatial and temporal differences of NG2 cell distribution were examined in several brain areas. For the stratum radiatum, stratum oriens, and corpus callosum, a decreasing density of NG2-expressing cells was found, entailing a more than 50% reduction of NG2-positive cells per area by P80–90. As opposed to this, NG2 expression remained constant in the dentate gyrus in all age groups with lower densities of NG2 glia altogether. The observed reduction of NG2-positive cells per area unit in most regions during aging implies that absolute cell numbers do not change significantly during this period, because the volume of the hippocampus roughly doubles in the period investigated (Zhang et al. 2005). Thus the halving of the density of NG2 glia between P10–12 and P25–35 in the stratum radiatum and stratum oriens is likely due to a doubling in the size of

the tissue between these ages leading to an almost constant overall number of NG2 glia. This is supported by the fact that in the dentate gyrus, which does not grow to the same extent as the other regions of the hippocampus, the number of NG2 glia remained unaltered.

NG2 glia may also generate oligodendrocytes which then become NG2-negative. However, in grey matter differentiation of NG2 glia into other cell types like oligodendrocytes is very low (Viagno and Dimou 2016). Furthermore, while NG2-cell densities decreased during the postnatal development, the density of astrocytes increases early postnatally and then remains stable with aging in the hippocampal CA1 region (Grosche et al. 2013; Nixdorf-Bergweiler et al. 1994; Schreiner et al. 2014).

Heterogeneity in NG2/S100 β labelling

Using immunohistochemistry, we also obtained clear evidence for the expression of S100 β in a subset of NG2 glia. Expression of S100 β by NG2 glia was first reported about a decade ago (Deloulme et al. 2004; Jabs et al. 2005; Matthias et al. 2003). More recently, the expression of S100 β by a subset of NG2 glia was shown at the transcriptional level (Haberlandt et al. 2011), but the frequency as well as the spatio-temporal development in the proportion of NG2 glia expressing S100 β remained a matter of debate. Numbers indeed strongly varied between different reports, reaching from no co-expression at all (Nishiyama et al. 1996) to 100 % co-expression (Deloulme et al. 2004).

The large differences between different reports might, at least partly, result from the use of different mouse strains and antibodies. Deloulme et al. (2004), who used immunocytochemistry and reported almost 100 % of co-localization of NG2 and S100 β in adult murine brain, employed an antibody which also recognizes other calcium binding proteins due to their sequence similarity (Bhattacharya et al. 2004; Isobe and Okuyama 1978). The antibody employed in the present study, however, exhibits a high specificity for S100 β as demonstrated above.

Our study revealed profound differences in the co-expression of S100 β and NG2 depending on the brain region and developmental stage. In the stratum radiatum and stratum oriens of the CA1 area, co-expression was strongest at P25–25, reaching 27 and 14 %, respectively. Interestingly, the amount decreased again in the stratum radiatum of adults to almost the same co-localization level as in P10–12, whereas it remained constant in the stratum oriens. In the dentate gyrus and corpus callosum, the co-expression level was initially low and did not vary between age groups.

These findings are partially consistent with those reported by Karram et al. (2008). In the latter study, approximately 20 % of NG2 glia in the hippocampus expressed S100 β in juvenile mice (P9–12) and 32 % in

adult animals (P75). For the corpus callosum, the co-expression was 26 and 32 % respectively. Hence, compared to what was found in the present study, S100 β expression of NG2 glia is similar in hippocampus of younger mice, whereas the values for adult mice differ. This discrepancy may result from the different methodological approaches which were employed to assess co-expression. Karram et al. (2008) used heterozygous EYFP mice when examining the expression of NG2-specific proteins, while here, direct labelling of the proteoglycan was performed. Notwithstanding, both reports coincide in showing that the majority of NG2 glia are devoid of S100 β , indicating that cells co-expressing both proteins represent a subtype of NG2 glia.

The exact functions of S100 β in NG2 glia are still unknown. On the one hand side, the S100 β protein in astroglia impacts neuronal neurite outgrowth (Azmitia et al. 1990; Liu and Lauder 1992) and may influence synaptic activity (Nishiyama et al. 2002b). On the other hand side, NG2 glia form synapses with neurons (Bergles et al. 2010), and synapses influence the fate of NG2 glia (Yang et al. 2013). These results suggest that expression of S100 β by NG2 glia may play a pivotal role in the formation and modulation of synapses between NG2 glia and neurons. Moreover, the subpopulation of cells co-expressing NG2 and S100 β may act as precursors for newly generated astrocytes and therefore support the postulated heterogeneity among NG2 glia. It has been shown earlier that subsets of NG2 glia may generate not only oligodendrocytes but also astroglia (Dimou et al. 2008; Trotter et al. 2010; Zhu et al. 2008). The NG2 cell fate was, and currently still is, a highly debated topic. While the oligodendrocyte precursor trait of NG2 glia has been firmly established (Nishiyama et al. 1996), contradicting results exist concerning the *in vivo* generation of astrocytes, as well as neurons (Belachew et al. 2003; Zhu et al. 2008). Recent fate mapping studies using different transgenic mice lines suggest that only prenatal NG2 glia may generate astrocytes (Dimou and Gallo 2015; Dimou and Wegner 2015; Huang et al. 2014; Kang et al. 2010; Rivers et al. 2008).

Proliferative potential of NG2/S100 β -positive cells

S100 β has been described as a marker for mature astroglia in the hippocampus (Seri et al. 2004; Steiner et al. 2004). Thus, our finding that this Ca²⁺-binding protein is also expressed in cells initially reported as precursor cells, is quite unexpected. This raises the question if expression of S100 β in the putative subgroup is linked to a particular cell fate. For this purpose, the expression of the proliferation marker Ki-67 was explored in NG2/S100 β -positive cells of the stratum radiatum, where co-expression of the two glial markers was maximal.

The protein Ki-67 is expressed almost exclusively in the interphase (G1, S, G2) and during mitosis, but not in the resting phase (G0), and is therefore a widely used antigen for proliferating cells (Bullwinkel et al. 2006). We observed no S100 β -positive NG2 negative cells (which are most likely astrocytes) expressing Ki-67. This observation is consistent with the notion that S100 β -expressing astrocytes are mature and are not in the cell cycle (Steiner et al. 2004). In contrast to astrocytes, the NG2 glial cells expressing S100 β have proliferative activity, at least at P25–35 and P85–95. In these time windows, the percentage of dividing cells was not lower than in S100 β -negative NG2 glia. This indicates that for NG2 glia, S100 β expression is not a sign of a mature, non-dividing cell.

Conclusions

We found a developmental increase in the expression of inwardly rectifying K⁺ channels, resulting in higher current densities, lower rectification indices and lower membrane resistances. We then tested if NG2 glia are heterogeneous with regard to their transcript and protein expression profiles. By employing RT-PCR analyses we found that the different glial genes are expressed at a variable extent across NG2 glia, independent of developmental stage and genetic background. At the protein level, all NG2 glial cells co-expressed PDGFR α , but in terms of other proteins they represented a rather heterogeneous population (Chittajallu et al. 2004; Karram et al. 2008; Mallon et al. 2002). In the current study we analyzed the S100 β expression by NG2 glia and observed regional as well as temporal heterogeneity. Additionally we observed that S100 β -positive NG2 glia have proliferative activity which is in contrast to S100 β -expressing astrocytes (Steiner et al. 2004). The exact function of S100 β in NG2 glia is still unclear, but since S100 β is important for neurite outgrowth (Azmitia et al. 1990; Liu and Lauder 1992) and influences neuronal synaptic activity (Nishiyama et al. 2002b), its expression, rather than that of the NG2 proteoglycan (Passlick et al. 2016), may be important for synapse formation between neurons and NG2 glia.

Acknowledgments We wish to thank Simone Durry for expert technical assistance. Supported by the Deutsche Forschungsgemeinschaft (DFG) (Ro 2327/8-1; SE 774/6; STE 552/4).

References

Asher RA, Morgenstern DA, Properzi F, Nishiyama A, Levine JM, Fawcett JW (2005) Two separate metalloproteinase activities are responsible for the shedding and processing of the NG2

- proteoglycan *in vitro*. *Mol Cell Neurosci* 29:82–96. doi:10.1016/j.mcn.2005.02.001
- Azmitia EC, Dolan K, Whitaker-Azmitia PM (1990) S-100B but not NGF, EGF, insulin or calmodulin is a CNS serotonergic growth factor. *Brain Res* 516:354–356
- Belachew S, Chittajallu R, Aguirre AA, Yuan X, Kirby M, Anderson S, Gallo V (2003) Postnatal NG2 proteoglycan-expressing progenitor cells are intrinsically multipotent and generate functional neurons. *J Cell Biol* 161:169–186. doi:10.1083/jcb.200210110
- Bergles DE, Roberts JD, Somogyi P, Jahr CE (2000) Glutamatergic synapses on oligodendrocyte precursor cells in the hippocampus. *Nature* 405:187–191. doi:10.1038/35012083
- Bergles DE, Jabs R, Steinhäuser C (2010) Neuron-glia synapses in the brain. *Brain Res Rev* 63:130–137. doi:10.1016/j.brainresrev.2009.12.003
- Berry M, Hubbard P, Butt AM (2002) Cytology and lineage of NG2-positive glia. *J Neurocytol* 31:457–467
- Bhattacharya S, Bunick CG, Chazin WJ (2004) Target selectivity in EF-hand calcium binding proteins. *Biochim Biophys Acta* 1742:69–79. doi:10.1016/j.bbamcr.2004.09.002
- Bordey A, Sontheimer H (1997) Postnatal development of ionic currents in rat hippocampal astrocytes *in situ*. *J Neurophysiol* 78:461–477
- Bullwinkel J, Baron-Luhr B, Ludemann A, Wohlenberg C, Gerdes J, Scholzen T (2006) Ki-67 protein is associated with ribosomal RNA transcription in quiescent and proliferating cells. *J Cell Physiol* 206:624–635. doi:10.1002/jcp.20494
- Butt AM, Hamilton N, Hubbard P, Pugh M, Ibrahim M (2005) Synantocytes: the fifth element. *J Anat* 207:695–706. doi:10.1111/j.1469-7580.2005.00458.x
- Chen PH, Cai WQ, Wang LY, Deng QY (2008) A morphological and electrophysiological study on the postnatal development of oligodendrocyte precursor cells in the rat brain. *Brain Res* 1243:27–37. doi:10.1016/j.brainres.2008.09.029
- Chittajallu R, Aguirre A, Gallo V (2004) NG2-positive cells in the mouse white and grey matter display distinct physiological properties. *J Physiol* 561:109–122. doi:10.1113/jphysiol.2004.074252
- Dawson MR, Polito A, Levine JM, Reynolds R (2003) NG2-expressing glial progenitor cells: an abundant and widespread population of cycling cells in the adult rat CNS. *Mol Cell Neurosci* 24:476–488
- Deloulme JC, Raponi E, Gentil BJ, Bertacchi N, Marks A, Labourdette G, Baudier J (2004) Nuclear expression of S100B in oligodendrocyte progenitor cells correlates with differentiation toward the oligodendroglial lineage and modulates oligodendrocytes maturation. *Mol Cell Neurosci* 27:453–465. doi:10.1016/j.mcn.2004.07.008
- Dimou L, Gallo V (2015) NG2-glia and their functions in the central nervous system. *Glia* 63:1429–1451. doi:10.1002/glia.22859
- Dimou L, Wegner M (2015) Oligodendroglial heterogeneity in time and space (NG2 glia in the CNS). *e-Neuroforum* 6:69–72. doi:10.1007/s13295-015-0010-2
- Dimou L, Simon C, Kirchhoff F, Takebayashi H, Gotz M (2008) Progeny of Olig2-expressing progenitors in the gray and white matter of the adult mouse cerebral cortex. *J Neurosci* 28:10434–10442. doi:10.1523/JNEUROSCI.2831-08.2008
- Djukic B, Casper KB, Philpot BD, Chin LS, McCarthy KD (2007) Conditional knock-out of Kir4.1 leads to glial membrane depolarization, inhibition of potassium and glutamate uptake, and enhanced short-term synaptic potentiation. *J Neurosci* 27:11354–11365. doi:10.1523/JNEUROSCI.0723-07.2007
- Donato R, Cannon BR, Sorci G, Riuzzi F, Hsu K, Weber DJ, Geczy CL (2013) Functions of S100 proteins. *Curr Mol Med* 13:24–57

- Gebara E et al (2016) Heterogeneity of radial Glia-like cells in the adult hippocampus. *Stem Cells*. doi:[10.1002/stem.2266](https://doi.org/10.1002/stem.2266)
- Grosche A et al (2013) Versatile and simple approach to determine astrocyte territories in mouse neocortex and hippocampus. *PLoS One* 8:e69143. doi:[10.1371/journal.pone.0069143](https://doi.org/10.1371/journal.pone.0069143)
- Haberlandt C et al (2011) Gray matter NG2 cells display multiple Ca^{2+} -signaling pathways and highly motile processes. *PLoS One* 6:e17575. doi:[10.1371/journal.pone.0017575](https://doi.org/10.1371/journal.pone.0017575)
- Hachem S, Aguirre A, Vives V, Marks A, Gallo V, Legraverend C (2005) Spatial and temporal expression of S100B in cells of oligodendrocyte lineage. *Glia* 51:81–97. doi:[10.1002/glia.20184](https://doi.org/10.1002/glia.20184)
- Horner PJ, Thallmair M, Gage FH (2002) Defining the NG2-expressing cell of the adult CNS. *J Neurocytol* 31:469–480
- Huang W et al (2014) Novel NG2-CreERT2 knock-in mice demonstrate heterogeneous differentiation potential of NG2 glia during development. *Glia* 62:896–913. doi:[10.1002/glia.22648](https://doi.org/10.1002/glia.22648)
- Isobe T, Okuyama T (1978) The amino-acid sequence of S-100 protein (PAP I-b protein) and its relation to the calcium-binding proteins. *Eur J Biochem FEBS* 89:379–388
- Jabs R, Pivneva T, Huttmann K, Wyczynski A, Nolte C, Kettenmann H, Steinhäuser C (2005) Synaptic transmission onto hippocampal glial cells with hGFAP promoter activity. *J Cell Sci* 118:3791–3803. doi:[10.1242/jcs.02515](https://doi.org/10.1242/jcs.02515)
- Kang SH, Fukaya M, Yang JK, Rothstein JD, Bergles DE (2010) NG2+ CNS glial progenitors remain committed to the oligodendrocyte lineage in postnatal life and following neurodegeneration. *Neuron* 68:668–681. doi:[10.1016/j.neuron.2010.09.009](https://doi.org/10.1016/j.neuron.2010.09.009)
- Karram K et al (2008) NG2-expressing cells in the nervous system revealed by the NG2-EYFP-knockin mouse. *Genesis* 46:743–757. doi:[10.1002/dvg.20440](https://doi.org/10.1002/dvg.20440)
- Kressin K, Kuprijanova E, Jabs R, Seifert G, Steinhäuser C (1995) Developmental regulation of Na^{+} and K^{+} conductances in glial cells of mouse hippocampal brain slices. *Glia* 15:173–187. doi:[10.1002/glia.440150210](https://doi.org/10.1002/glia.440150210)
- Kukley M, Kiladze M, Tognatta R, Hans M, Swandulla D, Schramm J, Dietrich D (2008) Glial cells are born with synapses. *FASEB J* 22(8):2957–2969. doi:[10.1096/fj.07-090985](https://doi.org/10.1096/fj.07-090985)
- Levine JM, Stallcup WB (1987) Plasticity of developing cerebellar cells in vitro studied with antibodies against the NG2 antigen. *J Neurosci* 7:2721–2731
- Levine JM, Reynolds R, Fawcett JW (2001) The oligodendrocyte precursor cell in health and disease. *Trends Neurosci* 24:39–47
- Lin SC, Bergles DE (2002) Physiological characteristics of NG2-expressing glial cells. *J Neurocytol* 31:537–549
- Liu JP, Lauder JM (1992) S-100 beta and insulin-like growth factor-II differentially regulate growth of developing serotonin and dopamine neurons in vitro. *J Neurosci Res* 33:248–256. doi:[10.1002/jnr.490330208](https://doi.org/10.1002/jnr.490330208)
- Maldonado PP, Velez-Fort M, Levavasseur F, Angulo MC (2013) Oligodendrocyte precursor cells are accurate sensors of local K^{+} in mature gray matter. *J Neurosci* 33:2432–2442. doi:[10.1523/JNEUROSCI.1961-12.2013](https://doi.org/10.1523/JNEUROSCI.1961-12.2013)
- Mallon BS, Shick HE, Kidd GJ, Macklin WB (2002) Proteolipid promoter activity distinguishes two populations of NG2-positive cells throughout neonatal cortical development. *J Neurosci* 22:876–885
- Matthias K, Kirchhoff F, Seifert G, Huttmann K, Matyash M, Kettenmann H, Steinhäuser C (2003) Segregated expression of AMPA-type glutamate receptors and glutamate transporters defines distinct astrocyte populations in the mouse hippocampus. *J Neurosci* 23:1750–1758
- Nishiyama A, Lin XH, Giese N, Heldin CH, Stallcup WB (1996) Colocalization of NG2 proteoglycan and PDGF alpha-receptor on O2A progenitor cells in the developing rat brain. *J Neurosci Res* 43:299–314. doi:[10.1002/\(SICI\)1097-4547\(19960201\)43:3<299:AID-JNR5>3.0.CO;2-E](https://doi.org/10.1002/(SICI)1097-4547(19960201)43:3<299:AID-JNR5>3.0.CO;2-E)
- Nishiyama A, Chang A, Trapp BD (1999) NG2+ glial cells: a novel glial cell population in the adult brain. *J Neuropathol Exp Neurol* 58:1113–1124
- Nishiyama A, Watanabe M, Yang Z, Bu J (2002a) Identity, distribution, and development of polydendrocytes: NG2-expressing glial cells. *J Neurocytol* 31:437–455
- Nishiyama H, Knopfel T, Endo S, Itohara S (2002b) Glial protein S100B modulates long-term neuronal synaptic plasticity. *Proc Natl Acad Sci USA* 99:4037–4042. doi:[10.1073/pnas.052020999](https://doi.org/10.1073/pnas.052020999)
- Nishiyama A, Komitova M, Suzuki R, Zhu X (2009) Polydendrocytes (NG2 cells): multifunctional cells with lineage plasticity. *Nat Rev Neurosci* 10:9–22. doi:[10.1038/nrn2495](https://doi.org/10.1038/nrn2495)
- Nixdorf-Bergweiler BE, Albrecht D, Heinemann U (1994) Developmental changes in the number, size, and orientation of GFAP-positive cells in the CA1 region of rat hippocampus. *Glia* 12:180–195. doi:[10.1002/glia.440120304](https://doi.org/10.1002/glia.440120304)
- Nolte C, Matyash M, Pivneva T, Schipke CG, Ohlemeyer C, Hanisch UK, Kirchhoff F, Kettenmann H (2001) GFAP promoter-controlled EGFP-expressing transgenic mice: a tool to visualize astrocytes and astrogliosis in living brain tissue. *Glia* 33:72–86. doi:[10.1002/1098-1136\(20010101\)33:1<72:AID-GLIA1007>3.0.CO;2-A](https://doi.org/10.1002/1098-1136(20010101)33:1<72:AID-GLIA1007>3.0.CO;2-A)
- Passlick S, Trotter J, Seifert G, Steinhäuser C, Jabs R (2016) The NG2 protein is not required for glutamatergic neuron-NG2 cell synaptic signaling. *Cereb Cortex* 26:51–57. doi:[10.1093/cercor/bhu171](https://doi.org/10.1093/cercor/bhu171)
- Polito A, Reynolds R (2005) NG2-expressing cells as oligodendrocyte progenitors in the normal and demyelinated adult central nervous system. *J Anat* 207:707–716. doi:[10.1111/j.1469-7580.2005.00454.x](https://doi.org/10.1111/j.1469-7580.2005.00454.x)
- Raponi E, Agenes F, Delphin C, Assard N, Baudier J, Legraverend C, Deloulme JC (2007) S100B expression defines a state in which GFAP-expressing cells lose their neural stem cell potential and acquire a more mature developmental stage. *Glia* 55:165–177. doi:[10.1002/glia.20445](https://doi.org/10.1002/glia.20445)
- Rivers LE et al (2008) PDGFRA/NG2 glia generate myelinating oligodendrocytes and piriform projection neurons in adult mice. *Nat Neurosci* 11:1392–1401. doi:[10.1038/nn.2220](https://doi.org/10.1038/nn.2220)
- Schreiner AE, Durry S, Aida T, Stock MC, Rütther U, Tanaka K, Rose CR, Kafitz KW (2014) Laminar and subcellular heterogeneity of GLAST and GLT-1 immunoreactivity in the developing postnatal mouse hippocampus. *J Comp Neurol* 522:204–224. doi:[10.1002/cne.23450](https://doi.org/10.1002/cne.23450)
- Schröder W, Seifert G, Huttmann K, Hinterkeuser S, Steinhäuser C (2002) AMPA receptor-mediated modulation of inward rectifier K^{+} channels in astrocytes of mouse hippocampus. *Mol Cell Neurosci* 19:447–458. doi:[10.1006/mcne.2001.1080](https://doi.org/10.1006/mcne.2001.1080)
- Seifert G, Huttmann K, Binder DK, Hartmann C, Wyczynski A, Neusch C, Steinhäuser C (2009) Analysis of astroglial K^{+} channel expression in the developing hippocampus reveals a predominant role of the Kir4.1 subunit. *J Neurosci* 29:7474–7488. doi:[10.1523/JNEUROSCI.3790-08.2009](https://doi.org/10.1523/JNEUROSCI.3790-08.2009)
- Seri B, Garcia-Verdugo JM, Collado-Morente L, McEwen BS, Alvarez-Buylla A (2004) Cell types, lineage, and architecture of the germinal zone in the adult dentate gyrus. *J Comp Neurol* 478:359–378. doi:[10.1002/cne.20288](https://doi.org/10.1002/cne.20288)
- Solga AC, Gianino SM, Gutmann DH (2014) NG2-cells are not the cell of origin for murine neurofibromatosis-1 (Nf1) optic glioma. *Oncogene* 33:289–299. doi:[10.1038/onc.2012.580](https://doi.org/10.1038/onc.2012.580)
- Steiner B, Kronenberg G, Jessberger S, Brandt MD, Reuter K, Kempermann G (2004) Differential regulation of gliogenesis in the context of adult hippocampal neurogenesis in mice. *Glia* 46:41–52. doi:[10.1002/glia.10337](https://doi.org/10.1002/glia.10337)
- Steinhäuser C, Dietrich D (2015) Neuron-glia synapses in the brain: properties, diversity and functions of NG2 glia. *e-Neuroforum* 6:73–77. doi:[10.1007/s13295-015-0010-2](https://doi.org/10.1007/s13295-015-0010-2)

- Steinhäuser C, Kressin K, Kuprijanova E, Weber M, Seifert G (1994) Properties of voltage-activated Na⁺ and K⁺ currents in mouse hippocampal glial cells in situ and after acute isolation from tissue slices. *Pflugers Arch* 428:610–620
- Trotter J, Karram K, Nishiyama A (2010) NG2 cells: properties, progeny and origin. *Brain Res Rev* 63:72–82. doi:[10.1016/j.brainresrev.2009.12.006](https://doi.org/10.1016/j.brainresrev.2009.12.006)
- Viagno F, Dimou L (2016) The heterogenous nature of NG2-glia. *Brain Res* 1638:129–137. doi:[10.1016/j.brainres.2015.09.012](https://doi.org/10.1016/j.brainres.2015.09.012)
- Wallraff A, Odermatt B, Willecke K, Steinhäuser C (2004) Distinct types of astroglial cells in the hippocampus differ in gap junction coupling. *Glia* 48:36–43. doi:[10.1002/glia.20040](https://doi.org/10.1002/glia.20040)
- Yang QK, Xiong JX, Yao ZX (2013) Neuron-NG2 cell synapses: novel functions for regulating NG2 cell proliferation and differentiation. *Biomed Res Int* 2013:402843. doi:[10.1155/2013/402843](https://doi.org/10.1155/2013/402843)
- Yuan X, Chittajallu R, Belachew S, Anderson S, McBain CJ, Gallo V (2002) Expression of the green fluorescent protein in the oligodendrocyte lineage: a transgenic mouse for developmental and physiological studies. *J Neurosci Res* 70:529–545. doi:[10.1002/jnr.10368](https://doi.org/10.1002/jnr.10368)
- Zhang J, Miller MI, Plachez C, Richards LJ, Yarowsky P, van Zijl P, Mori S (2005) Mapping postnatal mouse brain development with diffusion tensor microimaging. *Neuroimage* 26:1042–1051. doi:[10.1016/j.neuroimage.2005.03.009](https://doi.org/10.1016/j.neuroimage.2005.03.009)
- Zhu X, Bergles DE, Nishiyama A (2008) NG2 cells generate both oligodendrocytes and gray matter astrocytes. *Development* 135:145–157. doi:[10.1242/dev.004895](https://doi.org/10.1242/dev.004895)
- Zonouzi M et al (2015) GABAergic regulation of cerebellar NG2 cell development is altered in perinatal white matter injury. *Nat Neurosci* 18:674–682. doi:[10.1038/nn.3990](https://doi.org/10.1038/nn.3990)